PERGAMON

International Journal of Solids and Structures 37 (2000) 5995–6010

INTERNATIONAL JOURNAL OF SOLIDS and STRUCTURES

www.elsevier.com/locate/ijsolstr

# Non-existence of separable crack tip field in mechanism-based strain gradient plasticity

M.X. Shi[a], Y. Huang[a,*], H. Gao[b], K.C. Hwang[c]

[a]*Department of Mechanical and Industrial Engineering, University of Illinois at Urbana-Champaign, Urbana, IL 61801, USA*
[b]*Division of Mechanics and Computation, Stanford University, Stanford, CA 94305, USA*
[c]*Department of Engineering Mechanics, Tsinghua University, Beijing 100084, People's Republic of China*

Received 20 April 1999; in revised form 28 July 1999

**Abstract**

We investigate the structure of asymptotic crack tip fields associated with the recently developed theory of mechanism-based strain gradient (MSG) plasticity. The MSG plasticity theory directly connects micron scale plasticity to dislocation theories via a multiscale, hierarchical framework linking Taylor's dislocation hardening model to strain gradient plasticity. We show that the crack tip field in MSG plasticity does not have a separable form of solution. In contrast, all previously known asymptotic fields around stationary crack tips have separable form of solutions such as the classical $K$ field, HRR field, crack tip field in the couple stress theory of strain gradient plasticity, and the crack tip field in the Fleck–Hutchinson phenomenological theory of strain gradient plasticity. The physical significance of this lack of separable solution of the crack tip field in MSG plasticity is that stresses at a distance on the order of dislocation spacing from a crack tip can no longer be characterized by a single parameter as in classical $J$-controlled crack tip fields. This difficulty can be overcome by combining MSG plasticity theory with a cohesive model of fracture. 

*Keywords:* Crack tip field; Mechanism-based strain gradient plasticity

## 1. Introduction

### 1.1. Crack tip field in classical plasticity

The pioneering work of HRR field (Hutchinson, 1968; Rice and Rosengren, 1968) and $J$-integral (Rice, 1968) has laid the foundation of nonlinear fracture mechanics. For an elastic-power law hardening solid, the HRR field gives the stresses near a mode I crack tip as

* Corresponding author. Tel.: +1-217-265-5072; fax: +1-217-244-6534.
*E-mail address:* huang9@uiuc.edu (Y. Huang).

0020-7683/00/$ - see front matter 
PII: S0020-7683(99)00217-6

$$\sigma_{ij} = \left(\frac{J}{r}\right)^{1/(n+1)} \tilde{\sigma}_{ij}(\theta, n), \tag{1}$$

where $n$ is the plastic work hardening exponent, $(r, \theta)$ are polar coordinates centered at the crack tip, $\tilde{\sigma}_{ij}(\theta, n)$ are universal functions of polar angle $\theta$ (and $n$), and $J$ is the path-independent $J$-integral (Rice, 1968). It is observed that the $J$-integral is the only parameter that depends on external loading and specimen geometry, therefore, it governs the amplitude of stress field near the crack tip. Moreover, $J$ has been shown to be the crack tip energy release rate. Accordingly, the crack tip field is called the $J$-controlled field, and the fracture criterion becomes naturally the attainment of a critical value of $J$, i.e.,

$$J = J_{\mathrm{IC}}, \tag{2}$$

where $J_{\mathrm{IC}}$ is the critical value of $J$ for crack propagation and is related to fracture toughness $K_{\mathrm{IC}}$ by $J_{\mathrm{IC}} = K_{\mathrm{IC}}^2/E$ ($E$ is the Young's modulus).

The establishment of Eqs. (1) and (2) forms the foundation of nonlinear fracture mechanics. The mechanics and material aspects of nonlinear fracture mechanics can be summarized as:

1. the calculation of $J$ for various specimen and loading, and the determination of the dominance zone of crack tip field (in order to ensure the $J$-controlled crack tip field exists); and
2. the measurement of $J_{\mathrm{IC}}$ for various materials.

Significant effort has been made on these two separated aspects, and nonlinear fracture mechanics based on classical plasticity theories has been successfully applied to macroscopic fracture problems (e.g., Kannien and Popelar, 1985).

### *1.2. Strain gradient plasticity*

Although attempts have been made to link macroscopic cracking to atomistic fracture, they are frustrated by the inability of classical plasticity theories to model stress–strain behavior adequately at the small scales involved in crack tip deformation. For example, Elssner et al. (1994) have measured both the macroscopic fracture toughness and atomic work of separation of an interface between a single crystal of niobium and a sapphire single crystal. The interface between the two materials remains atomistically sharp, i.e., the crack tip is not blunted even though niobium has a large number of dislocations. The stress level needed to produce atomic decohesion of a lattice or a strong interface is typically on the order of 0.03 times of Young's modulus, or 10 times the tensile yield stress. However, as Hutchinson (1997) has pointed out, the maximum stress level that can be achieved near a crack tip is not larger than 4–5 times the tensile yield stress of metals, according to models based on classical plasticity theories. This clearly falls short triggering the atomic decohesion observed in Elssner et al.'s (1994) experiments.

Besides the inability to model stress–strain behavior adequately near a crack tip, classical plasticity theories, which possess no internal constitutive length parameters, also fail to predict the strong size effects ductile materials display in micro-indentation or nano-indentation hardness tests (e.g., Nix, 1989, 1997; de Guzman et al., 1993; Stelmashenko et al., 1993; Atkinson, 1995; Ma and Clarke, 1995; Poole et al., 1996; McElhaney et al., 1998); in micro-torsion of thin wires (Fleck et al., 1994); and in micro-bending of thin beams (Stolken and Evans, 1998). Frustrated by the inability of classical plasticity theories to model stress–strain behavior adequately at the small scale, Fleck and Hutchinson (1993, 1997) and Fleck et al. (1994) have developed a phenomenological theory of strain gradient plasticity intended for application to materials and structures whose dimension controlling plastic deformation ranges roughly from 0.1 to 10 μm. The theory is motivated by the dislocation analysis that the gradients of plastic shear are directly related to geometrically necessary dislocations in a material (Nye, 1953;

Cottrell, 1964; Ashby, 1970). The theory is a generalization of classical plasticity theories by incorporating strain gradients in the constitutive relation. At a relative large characteristic length scale (e.g., over 100 μm) associated with plastic deformation, plastic work hardening results mainly from the storage of statistically stored dislocations (Ashby, 1970) such that the theory degenerates to classical plasticity. As the characteristic length becomes small, however, geometrically necessary dislocations come into play and the material is further work hardened, in addition to that from statistically stored dislocations. This is consistent with the increase of strength at the micron scale in materials, as observed in aforementioned micro-indentation, micro-torsion and micro-bending experiments.

Some internal length parameters have been introduced in strain gradient plasticity in order to balance the dimensions of strains and strain gradients in the constitutive relation. Fleck and Hutchinson (1993) and Fleck et al. (1994) have introduced an internal constitutive length parameter to scale the rotation gradients in the couple stress theory of strain gradient plasticity. This length parameter is approximately 4 μm for copper from (Fleck et al., 1994) micro-torsion experiments, and 6 μm for nickel from Stolken and Evans' (1998) micro-bending experiments. However, the couple stress theory of strain gradient plasticity (Fleck and Hutchinson, 1993; Fleck et al., 1994) predicts only 10–20% increase in hardness (Shu and Fleck, 1998), which clearly falls short of agreement with the significant increase of 200–300% observed in micro-indentation or nano-indentation tests (e.g., Nix, 1989, 1997; de Guzman et al., 1993; Stelmashenko et al., 1993; Atkinson, 1995; Ma and Clarke, 1995; Poole et al., 1996; McElhaney et al., 1998). For this reason, Fleck and Hutchinson (1997) have extended the theory of strain gradient plasticity to include both rotation gradients and stretch gradients of deformation in the constitutive model. Accordingly, two additional internal material lengths have been introduced. By fitting indentation data, Begley and Hutchinson (1998) have determined that the new material length scaling the stretch gradients ranges from 0.22 to 0.6 μm.

There are also other alternative frameworks of strain gradient plasticity. Dai and Parks (1998) and Acharya and Bassani (1999) have considered possible formulations of strain gradient plasticity which retain the essential structure of classical plasticity and obey the Clausius–Duhem thermodynamic restrictions. They have concluded that the only possible formulation is a flow theory with strain gradients represented as internal variables which act to increase the current tangent modulus of plastic work hardening. However, there has not been a systematic way of constructing the tangent modulus so as to valid the framework.

The aforementioned strain gradient plasticity theories (Fleck and Hutchinson, 1993, 1997; Fleck et al., 1994; Dai and Parks, 1998; Acharya and Bassani, 1999) are motivated by dislocation theories. However, dislocation theories are not actually used to construct the theory of strain gradient plasticity. Instead, these strain gradient plasticity theories are developed primarily based on the macroscopically measured uniaxial stress–strain behavior, with one or several constitutive length parameter(s) to be determined. Micromechanical experiments such as micro-indentation, micro-torsion and micro-bending are used to fit these internal constitutive material lengths. In order to directly connect strain gradient plasticity to dislocation theories, Gao et al. (1999) and Huang et al. (1999c) have developed a theory of mechanism-based strain gradient (MSG) plasticity based on a multiscale, hierarchical framework. Taylor's dislocation model for plastic work hardening has been used as the building block for MSG plasticity. The microscale density of geometrically necessary dislocations has been related to the macroscale effective strain gradient through the Burger's vector of the material. This hierarchical structure provides a systematic approach for constructing the constitutive law of strain gradient plasticity by averaging Taylor's dislocation model over a representative cell. Although the new theory fits nicely within the mathematical framework of the phenomenological theory by Fleck and Hutchinson (1997), the new theory differs from all existing phenomenological theories in its mechanism-based guiding principles. As a result, the internal constitutive lengths in strain gradient plasticity have been determined as $(\mu/\sigma_{\text{ref}})^2 b$, rather than treated as fitting parameters, where $\mu$ is the shear modulus, $b$ is the Burger's vector, and $\sigma_{\text{ref}}$

is a reference stress (e.g., yield stress) in uniaxial tension. For typical ductile materials, these internal constitutive lengths are indeed of the order of microns.

It should be pointed out that, even though other dislocation models can also be used as the building block to construct strain gradient plasticity, we use Taylor's model because it is simple and robust. Moreover, as seen from Fig. 1, Nix and Gao (1998) have shown that the micro-indentation hardness predicted by strain gradient plasticity with Taylor's model agrees remarkably well with the micro-indentation experiments for various single crystal and polycrystal metals.

### *1.3. Fracture in strain gradient plasticity*

Classical plasticity falls short to give the large stresses needed for cleavage cracks in ductile materials as in (Elssner et al.'s, 1994) experiments. Strain gradient plasticity theories, however, may provide such a link between macroscopic cracking and atomistic fracture processes. Due to large strain gradients near a crack tip, stresses may be significantly larger than those in classical plasticity. Huang et al. (1995, 1997a, 1997b, 1999a), Xia and Hutchinson (1996), Wei and Hutchinson (1997) and Chen et al. (1998, 1999) have investigated the asymptotic field near a crack tip as well as the full-field solution. It is established that, for the couple stress theory of strain gradient plasticity (Fleck and Hutchinson, 1993, Fleck et al., 1994), the stress level near a crack tip is not significantly increased as compared to that in classical plasticity (Huang et al., 1995, 1997a, 1997b, 1999a; Xia and Hutchinson, 1996; Chen et al., 1998). This is because the effect of stretch gradients, which is important near a crack tip, has not been accounted for. In order to incorporate this effect, Chen et al. (1999) have used Fleck and Hutchinson's (Fleck and Hutchinson, 1997) phenomenological strain gradient plasticity theory that incorporates both the rotation and stretch gradients of deformation. Indeed, stretch gradients can elevate the stress level near a crack tip, as also observed in steady-state crack propagation (Wei and Hutchinson, 1997). However, Chen et al. (1999) have shown that the asymptotic crack tip field in (Fleck and Hutchinson's, 1997) phenomenological strain gradient plasticity gives an incorrect, compressive stress tractions ahead of a mode I crack tip. This is physically unacceptable since these compressive stress tractions are clearly against our physical intuition, and are opposite to those in classical $K$ field, HRR field, and the asymptotic crack tip field in the couple stress theory of strain gradient plasticity (Huang et al., 1995, 1997a, 1997b; Xia and Hutchinson, 1996). In order to solve this puzzle, Chen et al. (1999) have used the finite element method to obtain the full-field solution. They have established that this zone of

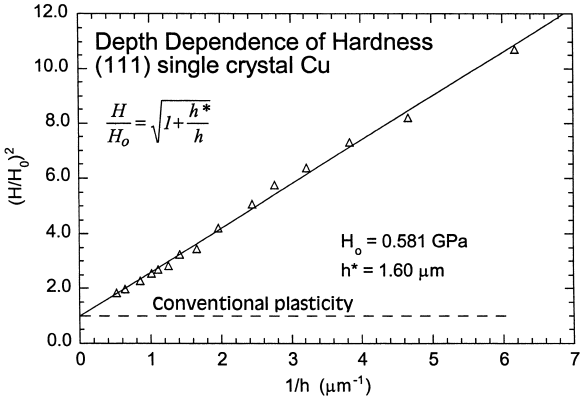


Fig. 1. Comparison of the experimentally measured depth dependence of the hardness of (111) single crystal copper with a strain gradient plasticity law based on the Taylor model (Nix and Gao, 1998).

compressive stress tractions is extremely small (less than 0.1 μm) and falls outside the intended range of applications (0.1–10 μm) for strain gradient plasticity. Therefore, the crack tip field in phenomenological strain gradient plasticity (Fleck and Hutchinson, 1997) has no domain of physical validity, i.e., the dominance zone of the asymptotic crack tip field vanishes. Accordingly, even though the path-independent $J$-integral exists in phenomenological strain gradient plasticity (Huang et al., 1995; Xia and Hutchinson, 1996), there is not a physically valid $J$-controlled crack tip field that has a universal form similar to that in Eq. (1).

In this paper, we investigate the crack tip field in MSG plasticity. The theory of MSG plasticity is summarized in Section 2. It is established in Section 3 that the crack tip field in MSG plasticity does not have a universal, separable form (with respect to $r$ and $\theta$) as in Eq. (1) for classical plasticity. Its implication on fracture in MSG plasticity is further discussed in Section 4.

## 2. Mechanism-based strain gradient (MSG) plasticity

The deformation theory of MSG plasticity (Gao et al., 1999; Huang et al., 1999c) is summarized in this section. It has incorporated the modifications recently proposed by Huang et al. (1999b) based on polycrystal plasticity.

### 2.1. Generalized stresses and strains

In a Cartesian reference frame $x_i$, the strain tensor $\epsilon_{ij}$ and strain gradient tensor $\eta_{ijk}$ are related to the displacement $u_i$ by

$$\epsilon_{ij} = \frac{1}{2}(u_{i,\,j} + u_{j,\,i}) \tag{3}$$

and

$$\eta_{ijk} = u_{k,\,ij}, \tag{4}$$

which have the symmetry $\epsilon_{ij} = \epsilon_{ji}$ and $\eta_{ijk} = \eta_{jik}$. The elastic deformation is neglected in the crack tip field. Therefore, the incompressibility gives

$$\epsilon_{ii} = 0, \quad \eta_{kii} = 0. \tag{5}$$

The work increment per unit volume of an incompressible solid due to a variation of displacement $\delta u_i$ is

$$\delta w = \sigma'_{ij}\delta\epsilon_{ij} + \tau'_{ijk}\delta\eta_{ijk}, \tag{6}$$

where the symmetric deviatoric Cauchy stress $\sigma'_{ij}$ is the work conjugate of the variation of strain $\delta\epsilon_{ij}$, and $\sigma'_{ii} = 0$; the symmetric deviatoric higher-order stress $\tau'_{ijk}$ is the work conjugate of the variation of strain gradient $\delta\eta_{ijk}$, and $\tau'_{kii} = 0$.

### 2.2. Equilibrium equations and boundary conditions

The equilibrium equations for an incompressible solid can be written as

$$\sigma'_{ik,\,i} - \tau'_{ijk,\,ij} + H_{,k} + f_k = 0, \tag{7}$$

where $f_k$ is the body force and $H$ is the combined measure of the hydrostatic stress and hydrostatic

higher-order stress and is given by

$$H = \frac{1}{3}\sigma_{kk} - \frac{1}{2}\tau_{jkk,\,j}. \tag{8}$$

The higher-order stress tractions $\hat{r}_k$ tangential to the surface of the body are

$$\hat{r}_k = n_i n_j \tau'_{ijk} - n_k n_i n_j n_p \tau'_{ijp}. \tag{9}$$

The stress tractions on the surface of the body are

$$\hat{t}_k = H n_k + n_i\left(\sigma'_{ik} - \tau'_{ijk,j}\right) + D_k\left(n_i n_j n_p \tau'_{ijp}\right) - D_j\left(n_i \tau'_{ijk}\right) + \left(n_i n_j \tau'_{ijk} - n_k n_i n_j n_p \tau'_{ijp}\right)\left(D_q n_q\right), \tag{10}$$

where $n_i$ is the unit normal to the surface and $D_j$ is the surface-gradient operator given by

$$D_j = \left(\delta_{jk} - n_j n_k\right)\frac{\partial}{\partial x_k}. \tag{11}$$

On the surface of the body, the gradient $\partial/\partial x_j$ can be resolved into the above surface gradient $D_j$ and a normal gradient $n_j D$, i.e.,

$$\frac{\partial}{\partial x_j} = D_j + n_j D, \tag{12}$$

where

$$D = n_k \frac{\partial}{\partial x_k}. \tag{13}$$

### 2.3. Constitutive equations

The uniaxial stress–strain relation can be written as

$$\sigma = \sigma_{\mathrm{ref}} f(\epsilon), \tag{14}$$

where $\sigma_{\mathrm{ref}}$ is a reference stress in uniaxial tension and $f$ is a function of strain. For most ductile materials, the function $f$ can be written as a power law relation

$$f(\epsilon) = \epsilon^N, \tag{15}$$

where $N$ is the plastic work hardening exponent ($0 \le N < 1$). The flow stress, after incorporating the strain gradient effects, is obtained from Taylor's dislocation model as

$$\sigma = \sigma_{\mathrm{ref}}\sqrt{f^{\,2}(\epsilon) + l\eta}, \tag{16}$$

where $\epsilon$ and $\eta$ are the effective strain and effective strain gradient, respectively,

$$\epsilon = \sqrt{\frac{2}{3}\epsilon_{ij}\epsilon_{ij}}, \qquad \eta = \frac{1}{2}\sqrt{\eta_{ijk}\eta_{ijk}}. \tag{17}$$

The term $l\eta$ represents the contribution from geometrically necessary dislocations, while the other term $f^{\,2}(\epsilon)$ represents the counterpart from statistically stored dislocations (Nix and Gao, 1998). The

characteristic material length $l$ for strain gradient plasticity in Eq. (16) is given in terms of shear modulus $\mu$ and Burger's vector $b$ by

$$l = M^2\alpha^2\left(\frac{\mu}{\sigma_{\text{ref}}}\right)^2 b, \tag{18}$$

where $\alpha$ is an empirical material constant in Taylor's dislocation model for plastic work hardening of ductile materials, and is of the order of 1 (e.g., Nix and Gibeling, 1985); $M$ is the ratio of tensile flow stress to shear flow stress, and $M = 3.06$ for polycrystals (Taylor, 1938; Kocks, 1970). Nix and Gao (1998) have used $M = \sqrt{3}$ based on the von Mises rule for isotropic solids. For ductile materials, the intrinsic material length $l$ at which strain gradient effects are important is indeed of the order of microns.

The constitutive equations for MSG plasticity are

$$\sigma'_{ij} = \frac{2\epsilon_{ij}}{3\epsilon}\sigma, \tag{19}$$

$$\tau'_{ijk} = l_\epsilon^2\left[\frac{\sigma}{\epsilon}\left(\Lambda_{ijk} - \Pi_{ijk}\right) + \frac{\sigma_{\text{ref}}^2 f(\epsilon)f'(\epsilon)}{\sigma}\Pi_{ijk}\right], \tag{20}$$

where the flow stress $\sigma$ is given in terms of the effective strain $\epsilon$ and effective strain gradient $\eta$ in Eq. (16), and $\Lambda_{ijk}$ and $\Pi_{ijk}$ are given by

$$\Lambda_{ijk} = \frac{1}{72}\left[2\eta_{ijk} + \eta_{kij} + \eta_{kji} - \frac{1}{4}\left(\delta_{ik}\eta_{ppj} + \delta_{jk}\eta_{ppi}\right)\right], \tag{21}$$

$$\Pi_{ijk} = \frac{1}{54}\frac{\epsilon_{mn}}{\epsilon^2}\left[\epsilon_{ik}\eta_{jmn} + \epsilon_{jk}\eta_{imn} - \frac{1}{4}\left(\delta_{ik}\epsilon_{jp} + \delta_{jk}\epsilon_{ip}\right)\eta_{pmn}\right]. \tag{22}$$

The length $l_\epsilon$ in Eq. (20) is the mesoscale cell size, which will be discussed in detail in Section 4. It is of the order of average dislocation spacing at plastic yielding, $L_{\text{yield}}$, i.e.,

$$l_\epsilon = \beta L_{\text{yield}} = \beta\frac{\mu}{\sigma_{\text{Y}}}b, \tag{23}$$

where $L_{\text{yield}} = \mu b/\sigma_{\text{Y}}$ is the mean spacing between statistically stored dislocations at plastic yielding, $\sigma_{\text{Y}}$ is the yield stress in uniaxial tension, and $\beta$ is a constant coefficient of the order of 10 (Huang et al., 1999b).

## 3. Crack tip field in MSG plasticity

Follow the HRR field (Hutchinson, 1968; Rice and Rosengren, 1968), we search for the asymptotic crack tip field that has a separable dependence on $r$ and $\theta$ as in Eq. (1). We begin with the mode III crack tip field.

### 3.1. Mode III crack tip field in MSG plasticity

An infinite medium with a semi-infinite crack is subjected to anti-plane shear. The Cartesian reference

frame is set such that the crack coincides with the negative $x_1$ axis, and the anti-plane shear is parallel to the $x_3$ axis. The only non-vanishing displacement is the out-of-plane displacement $u_3 = w(x_1, x_2)$. The polar coordinates $(r, \theta)$ are used in the near-tip asymptotic analysis. The displacement near the mode III crack tip is assumed to have a separable form, i.e.,

$$w = r^{\lambda}\tilde{w}(\theta), \tag{24}$$

where the power $\lambda$ and angular function $\tilde{w}(\theta)$ are to be determined. In order to ensure that the displacement is bounded in the singular crack tip field, the power $\lambda$ is limited in the range $0 < \lambda < 2$. (Neither strains nor strain gradients would be singular at the crack tip if $\lambda$ is larger than 2.) The non-vanishing strains and strain gradients in polar coordinates are

$$\epsilon_{r3} = \epsilon_{3r} = \frac{\lambda}{2} r^{\lambda-1}\tilde{w}, \quad \epsilon_{\theta 3} = \epsilon_{3\theta} = \frac{1}{2} r^{\lambda-1}\tilde{w}', \tag{25}$$

$$\eta_{rr3} = \lambda(\lambda-1) r^{\lambda-2}\tilde{w}, \quad \eta_{r\theta 3} = \eta_{\theta r3} = (\lambda-1) r^{\lambda-2}\tilde{w}', \quad \eta_{\theta\theta 3} = r^{\lambda-2}(\lambda\tilde{w} + \tilde{w}''). \tag{26}$$

The effective strain $\epsilon$ and effective strain gradient $\eta$ are given by

$$\epsilon = \frac{1}{\sqrt{3}} r^{\lambda-1}\sqrt{\lambda^2\tilde{w}^2 + \tilde{w}'^2}, \qquad \eta = \frac{1}{2} r^{\lambda-2}\sqrt{\lambda^2(\lambda-1)^2\tilde{w}^2 + 2(\lambda-1)^2\tilde{w}'^2 + (\lambda\tilde{w} + \tilde{w}'')^2}. \tag{27}$$

The flow stress $\sigma$, as given in Eq. (16), is composed of the uniaxial flow stress term $f(\epsilon)$ and the strain gradient term $l\eta$. From the strain and strain gradient in Eq. (27), it can be shown that the strain gradient term $l\eta$ is more singular than $f^{2}(\epsilon)$ in Eq. (16), and therefore, dominates the flow stress. The physical interpretation is that the density of geometrically necessary dislocation near a crack tip is much larger than that of statistically stored dislocations. Therefore, the dominant term in the flow stress $\sigma$ is given by

$$\sigma = \sqrt{3}\alpha\mu\sqrt{b\eta}. \tag{28}$$

It is observed that the above flow stress near a crack tip in MSG plasticity is independent of the uniaxial stress–strain behavior, $f(\epsilon)$, and therefore, is independent of the plastic work hardening exponent $N$. This is the direct result of the flow stress (16) in MSG plasticity, and it does not hold for the HRR field in classical plasticity, nor for the crack tip field in phenomenological strain gradient plasticity.

The deviatoric stresses and deviatoric higher-order stresses can be obtained from the constitutive equations (19) and (20). The non-vanishing stresses are

$$\sigma'_{r3} = \sigma'_{3r} = \frac{2\epsilon_{r3}}{3\epsilon}\sigma = r^{(\lambda/2)-1}\tilde{\sigma}'_{r3}(\theta), \quad \sigma'_{\theta 3} = \sigma'_{3\theta} = \frac{2\epsilon_{\theta 3}}{3\epsilon}\sigma = r^{(\lambda/2)-1}\tilde{\sigma}'_{\theta 3}(\theta), \tag{29}$$

where $\tilde{\sigma}'_{r3}(\theta)$ and $\tilde{\sigma}'_{\theta 3}(\theta)$ are angular functions for stresses. The higher-order stresses, as seen in Eq. (20), should depend on both the uniaxial stress–strain curve $f(\epsilon)$ and the strain gradient $\eta$ through the flow stress $\sigma$. However, terms associated with $f(\epsilon)$ are less singular than those associated with the flow stress $\sigma$. If only the dominating singular terms are kept in the asymptotic field around a crack tip, the non-vanishing singular higher-order stresses are

$$\tau'_{r\theta 3} = \tau'_{\theta r3} = \frac{l_\epsilon^2}{54}\frac{\sigma}{\epsilon}\left[ -\frac{\epsilon_{r3}\epsilon_{\theta 3}}{\epsilon^2}(\eta_{rr3} + \eta_{\theta\theta 3}) + \frac{3}{4}\eta_{r\theta 3}\right] = r^{(\lambda/2)-2}\tilde{\tau}'_{r\theta 3}(\theta),$$

$$\tau'_{\theta\theta3} = \frac{l_\epsilon^2}{54}\frac{\sigma}{\epsilon}\left[\left(\frac{3}{2} - 2\frac{\epsilon_{\theta3}^2}{\epsilon^2}\right)\eta_{\theta\theta3} - 2\frac{\epsilon_{r3}\epsilon_{\theta3}}{\epsilon^2}\eta_{r\theta3}\right] = r^{(\lambda/2)-2}\tilde{\tau}'_{\theta\theta3}(\theta),$$

$$\tau'_{3rr} = \tau'_{r3r} = \frac{l_\epsilon^2}{54}\frac{\sigma}{\epsilon}\left[\left(\frac{9}{16} - \frac{3\epsilon_{r3}^2}{4\epsilon^2}\right)\eta_{rr3} - \left(\frac{3}{16} - \frac{\epsilon_{\theta3}^2}{4\epsilon^2}\right)\eta_{\theta\theta3} - \frac{\epsilon_{r3}\epsilon_{\theta3}}{2\epsilon^2}\eta_{r\theta3}\right] = r^{(\lambda/2)-2}\tilde{\tau}'_{3rr}(\theta),$$

$$\tau'_{3\theta r} = \tau'_{\theta3r} = \frac{l_\epsilon^2}{54}\frac{\sigma}{\epsilon}\left[-\frac{\epsilon_{r3}\epsilon_{\theta3}}{\epsilon^2}\eta_{\theta\theta3} + \left(\frac{3}{4} - \frac{\epsilon_{r3}^2}{\epsilon^2}\right)\eta_{r\theta3}\right] = r^{(\lambda/2)-2}\tilde{\tau}'_{3\theta r}(\theta),$$

$$\tau'_{3\theta\theta} = \tau'_{\theta3\theta} = \frac{l_\epsilon^2}{54}\frac{\sigma}{\epsilon}\left[-\left(\frac{3}{16} - \frac{\epsilon_{r3}^2}{4\epsilon^2}\right)\eta_{rr3} + \left(\frac{9}{16} - \frac{3\epsilon_{\theta3}^2}{4\epsilon^2}\right)\eta_{\theta\theta3} - \frac{\epsilon_{r3}\epsilon_{\theta3}}{2\epsilon^2}\eta_{r\theta3}\right] = r^{(\lambda/2)-2}\tilde{\tau}'_{3\theta\theta}(\theta),$$

$$\tau'_{333} = -\frac{l_\epsilon^2}{108}\frac{\sigma}{\epsilon}\left[\left(\frac{3}{4} - \frac{\epsilon_{r3}^2}{\epsilon^2}\right)\eta_{rr3} + \left(\frac{3}{4} - \frac{\epsilon_{\theta3}^2}{\epsilon^2}\right)\eta_{\theta\theta3} - 2\frac{\epsilon_{r3}\epsilon_{\theta3}}{\epsilon^2}\eta_{r\theta3}\right] = r^{(\lambda/2)-2}\tilde{\tau}'_{333}(\theta), \tag{30}$$

where $l_\epsilon$ is the mesoscale cell size in Eq. (23).

The hydrostatic stress $H$ vanishes in an anti-plane shear problem. The substitution of stresses and higher-order stresses into the equilibrium equation (7) gives the governing equation for the angular distribution of displacement, $\tilde{w}(\theta)$,

$$\left(-\frac{3}{16}\frac{A'^2}{A^2} + \frac{1}{4}\frac{A''}{A} - \frac{3}{4}\frac{A'}{A}\frac{B'}{B} + \frac{15}{4}\frac{B'^2}{B^2} - \frac{3}{2}\frac{B''}{B} + 2 - \frac{\lambda}{2}\right)\lambda\tilde{w}C + \frac{2+3\lambda}{8}\left(\frac{A'}{A} - 6\frac{B'}{B}\right)\tilde{w}'C$$
$$+ \left(\frac{1}{2}\frac{A'}{A} - 3\frac{B'}{B}\right)\lambda\tilde{w}C' + \left(1 + \frac{\lambda}{2}\right)\tilde{w}''C + \left(1 + \frac{3\lambda}{2}\right)\tilde{w}'C' + \lambda\tilde{w}C'' = 0, \tag{31}$$

where $A$, $B$ and $C$ are given by

$$A = \lambda^2(\lambda-1)^2\tilde{w}^2 + 2(\lambda-1)^2\tilde{w}'^2 + (\lambda\tilde{w} + \tilde{w}'')^2,$$

$$B = \lambda^2\tilde{w}^2 + \tilde{w}'^2,$$

$$C = \lambda^2\tilde{w}^2 - (\lambda-1)\tilde{w}'^2 + \lambda\tilde{w}\tilde{w}''. \tag{32}$$

It is observed that Eq. (31) is a fourth-order ordinary differential equation. There are two anti-symmetry conditions ahead of the crack tip ($\theta = 0$) and two traction-free boundary conditions on the crack face, i.e.,

$$\tilde{w} = \tilde{w}'' = 0 \quad \text{at } \theta = 0 \tag{33}$$

and

$$\hat{r}_\theta = \hat{t}_\theta = 0 \quad \text{at } \theta = \pi, \tag{34}$$

which can be written in terms of the angular function $\tilde{w}$ as

$$\left[\lambda^2\tilde{w}^2-(\lambda-1)\tilde{w}'^{\,2}+\lambda\tilde{w}\tilde{w}''\right]_{\theta=\pi}=\left[2\lambda^2\tilde{w}\tilde{w}'+(2-\lambda)\tilde{w}'\tilde{w}''+\lambda\tilde{w}\tilde{w}'''\right]_{\theta=\pi}=0. \tag{35}$$

It should be emphasized that Eqs. (31)–(33) and (35) form an eigenvalue problem, with the power $\lambda$ as the eigenvalue to be determined. However, unlike the HRR field in classical plasticity (Hutchinson, 1968; Rice and Rosengren, 1968), the eigenvalue $\lambda$ is not known a priori. Without losing generality, we may use a normalization condition

$$\tilde{w}'=1 \quad \text{at } \theta=0. \tag{36}$$

It appears that a numerical method could be used to solve this ordinary differential equation, with the power $\lambda$ and $\tilde{w}'''(\theta=0)$ as the two parameters varying in order to satisfy two crack face traction-free boundary conditions in Eq. (35). However, the following simple analysis excludes the possibility of any solutions for the ordinary differential equation (31).

It is recalled that Eq. (31) is a fourth-order differential equation. In fact, after some algebraic calculations, we find that Eq. (31) can be rewritten as

$$\frac{\mathrm{d}^4\tilde{w}}{\mathrm{d}\theta^4}=\frac{g_1\left(\tilde{w},\tilde{w}',\tilde{w}'',\tilde{w}'''\right)}{g_2\left(\tilde{w},\tilde{w}',\tilde{w}''\right)}, \tag{37}$$

where, very importantly, the denominator $g_2$ vanishes when $\tilde{w}=\tilde{w}''=0$. It is observed that the left-hand side of Eq. (37) is zero at $\theta=0$ due to anti-symmetry in mode III. The right-hand side of Eq. (37), however, would approach infinity because the denominator would vanish. In fact, near $\theta=0$, $\tilde{w}$ can be expanded in a Taylor series of $\theta$ using the odd powers only. It can be shown that the left-hand side of Eq. (37) is of the order of $\theta$, and the denominator and numerator of the right-hand side are of the order of $\theta$ and $a_0+a_2\theta^2$, respectively, where $a_0$ and $a_2$ are constants depending on $\tilde{w}'(\theta=0)$ and $\tilde{w}'''(\theta=0)$. In order to match the power of $\theta$ on both sides of Eq. (37) near $\theta=0$, the only solution is to set the constant $a_0$ to zero. Therefore, $\tilde{w}'''(\theta=0)$ is not independent of $\tilde{w}'(\theta=0)$, such that there is only one parameter left, namely the power $\lambda$, to satisfy the two traction-free boundary conditions in Eq. (35). It is highly improbable for this problem to have solutions. In fact, we have used the numerical shooting method (Press et al., 1986) to explore the entire range of $\lambda$ and, indeed, no solutions can be found to satisfy the two boundary conditions in Eq. (35) on the crack faces. We have also searched for separable solutions in a much larger range of $\lambda$, $0<\lambda<6$, and still no solutions can be obtained.

We would like to point out that this requirement of bounded $\mathrm{d}^4\tilde{w}/\mathrm{d}\theta^4$ at $\theta=0$ gives an extra boundary condition, which makes this eigenvalue problem overly constrained, and therefore, has no solution. This extra boundary condition at $\theta=0$, however, results directly from the assumed separable form (24) in the asymptotic crack tip field. In fact, it can be shown that, for general displacement field $w(r,\theta)$, the coefficient of the highest-order derivative with respect to $\theta$, $\partial^4 w/\partial\theta^4$, in the equilibrium equation is not zero. Only when the displacement field $w$ takes the separable form in Eq. (24), the coefficient of $\partial^4 w/\partial\theta^4$ becomes the denominator $g_2$ in Eq. (37) and vanishes at $\theta=0$. Therefore, the displacement in the asymptotic crack tip field is non-separable.

### 3.2. Mode I and mode II crack tip fields in MSG plasticity

The asymptotic crack tip field is dominated by plastic deformation such that the deformation near a crack tip is incompressible. Accordingly, a displacement potential $\phi$ for plane strain is introduced as

$$u_r=-\frac{1}{r}\frac{\partial\phi}{\partial\theta}, \quad u_\theta=\frac{\partial\phi}{\partial r}, \tag{38}$$

where $(r,\theta)$ are polar coordinates centered at the crack tip and crack faces coincide with $\theta=\pm\pi$.

Similar to the HRR field in classical plasticity (Hutchinson, 1968; Rice and Rosengren, 1968), we look for a separable crack tip field in which the displacement potential can be written as

$$\phi = r^{\lambda+1}\tilde{\phi}(\theta), \tag{39}$$

where the power $\lambda$ and angular function $\tilde{\phi}(\theta)$ are to be determined. The displacements, strains and strain gradients can be obtained from the displacement potential (38) and kinematic relations (3) and (4) as

$$u_r = -r^{\lambda}\tilde{\phi}', \qquad u_\theta = (\lambda+1)r^{\lambda}\tilde{\phi}, \tag{40}$$

$$\epsilon_{rr} = -\epsilon_{\theta\theta} = -\lambda r^{\lambda-1}\tilde{\phi}', \quad \epsilon_{r\theta} = \epsilon_{\theta r} = \frac{1}{2}r^{\lambda-1}\Big[-\tilde{\phi}'' + \big(\lambda^2-1\big)\tilde{\phi}\Big], \tag{41}$$

$$\eta_{rrr} = -\eta_{r\theta\theta} = -\eta_{\theta r\theta} = -\lambda(\lambda-1)r^{\lambda-2}\tilde{\phi}',$$

$$\eta_{rr\theta} = \lambda\big(\lambda^2-1\big)r^{\lambda-2}\tilde{\phi},$$

$$\eta_{r\theta r} = \eta_{\theta rr} = -\eta_{\theta\theta\theta} = -(\lambda-1)r^{\lambda-2}\Big[\tilde{\phi}'' + (\lambda+1)\tilde{\phi}\Big],$$

$$\eta_{\theta\theta r} = -r^{\lambda-2}\Big[\tilde{\phi}''' + (3\lambda+1)\tilde{\phi}'\Big]. \tag{42}$$

In particular, strains and strain gradients can be generally written as

$$\epsilon_{\alpha\beta} = r^{\lambda-1}\tilde{\epsilon}_{\alpha\beta}(\theta), \qquad \eta_{\alpha\beta\gamma} = r^{\lambda-2}\tilde{\eta}_{\alpha\beta\gamma}(\theta). \tag{43}$$

The power $\lambda$ is between 0 and 2, $0 < \lambda < 2$, in order to ensure that the displacements are bounded in the *singular* crack tip field.

The effective strain $\epsilon$ and effective strain gradient $\eta$ are obtained from Eq. (17) as

$$\epsilon = r^{\lambda-1}\tilde{\epsilon}(\theta) = r^{\lambda-1}\sqrt{\frac{2}{3}\tilde{\epsilon}_{\alpha\beta}\tilde{\epsilon}_{\alpha\beta}}, \qquad \eta = r^{\lambda-2}\tilde{\eta}(\theta) = r^{\lambda-2}\frac{1}{2}\sqrt{\tilde{\eta}_{\alpha\beta\gamma}\tilde{\eta}_{\alpha\beta\gamma}}. \tag{44}$$

Similar to the mode III crack tip field in Section 3.1, the flow stress $\sigma$ given in Eq. (16) is dominated by the strain gradient term $l\eta$, i.e., the uniaxial flow stress term $f(\epsilon)$ is negligible. Its physical interpretation is again that the density of geometrically necessary dislocations is much larger than that of statistically stored dislocations near a crack tip. Accordingly, the flow stress near the crack tip is given by

$$\sigma = r^{(\lambda/2)-1}\tilde{\sigma}(\theta) = r^{(\lambda/2)-1}\sigma_Y\sqrt{l\tilde{\eta}}. \tag{45}$$

Similar to mode III in Section 3.1, the flow stress above near a crack tip in MSG plasticity is independent of the uniaxial stress–strain curve $f(\epsilon)$, and is therefore independent of the plastic work hardening exponent $N$. This once again results from the flow stress (16) in MSG plasticity, and it does not hold for the HRR field in classical plasticity, nor for the crack tip field in phenomenological strain gradient plasticity.

The deviatoric stresses can be obtained from Eq. (19) as

$$\sigma'_{\alpha\beta} = r^{(\lambda/2)-1}\tilde{\sigma}'_{\alpha\beta}(\theta) = r^{(\lambda/2)-1}\frac{2\tilde{\epsilon}_{\alpha\beta}}{3\tilde{\epsilon}}\tilde{\sigma}. \tag{46}$$

For deviatoric higher-order stresses given in (20), the term $\sigma_\chi^2 f(\epsilon)f'(\epsilon)/\sigma$ is less singular than $\sigma/\epsilon$ and becomes negligible. Therefore, the dominating higher-order stresses are

$$\tilde{\tau}'_{\alpha\beta\gamma} = r^{(\lambda/2)-2}\tilde{\tau}'_{\alpha\beta\gamma}(\theta) = r^{(\lambda/2)-2}l_\epsilon^2\frac{\tilde{\sigma}}{\tilde{\epsilon}}\Big[\tilde{\Lambda}_{\alpha\beta\gamma}(\theta) - \tilde{\Pi}_{\alpha\beta\gamma}(\theta)\Big], \tag{47}$$

where

$$\tilde{\Lambda}_{\alpha\beta\gamma}(\theta) = \frac{1}{72}\Big[2\tilde{\eta}_{\alpha\beta\gamma} + \tilde{\eta}_{\gamma\alpha\beta} + \tilde{\eta}_{\gamma\beta\alpha} - \frac{1}{4}\big(\delta_{\alpha\gamma}\tilde{\eta}_{\delta\delta\beta} + \delta_{\beta\gamma}\tilde{\eta}_{\delta\delta\alpha}\big)\Big], \tag{48}$$

$$\tilde{\Pi}_{\alpha\beta\gamma}(\theta) = \frac{1}{54}\frac{\tilde{\epsilon}_{\delta\lambda}}{\tilde{\epsilon}^2}\Big[\tilde{\epsilon}_{\alpha\gamma}\tilde{\eta}_{\beta\delta\lambda} + \tilde{\epsilon}_{\beta\gamma}\tilde{\eta}_{\alpha\delta\lambda} - \frac{1}{4}\big(\delta_{\alpha\gamma}\tilde{\epsilon}_{\beta\xi} + \delta_{\beta\gamma}\tilde{\epsilon}_{\alpha\xi}\big)\tilde{\eta}_{\xi\delta\lambda}\Big]. \tag{49}$$

It is observed that both deviatoric stresses and deviatoric higher-order stresses are independent of uniaxial stress–strain curve $f(\epsilon)$.

The substitution of stresses and higher-order stresses into the equilibrium equation (7) gives

$$\begin{aligned}
&\frac{\mathrm{d}^2\tilde{\tau}'_{\theta\theta r}}{\mathrm{d}\theta^2} + 2\left(\frac{\lambda}{2}-1\right)\frac{\mathrm{d}\tilde{\tau}'_{\theta rr}}{\mathrm{d}\theta} - 2\frac{\mathrm{d}\tilde{\tau}'_{\theta\theta\theta}}{\mathrm{d}\theta} + \left(\frac{\lambda}{2}-1\right)\left(\frac{\lambda}{2}-2\right)\tilde{\tau}'_{rrr}\\
&-2\left(\frac{\lambda}{2}-1\right)\tilde{\tau}'_{r\theta\theta} - \left(\frac{\lambda}{2}-1\right)\tilde{\tau}'_{\theta\theta r} - \left(\frac{\lambda}{2}-3\right)\tilde{H} = 0,\\
&\frac{\mathrm{d}^2\tilde{\tau}'_{\theta\theta\theta}}{\mathrm{d}\theta^2} + 2\left(\frac{\lambda}{2}-1\right)\frac{\mathrm{d}\tilde{\tau}'_{r\theta\theta}}{\mathrm{d}\theta} + 2\frac{\mathrm{d}\tilde{\tau}'_{\theta\theta r}}{\mathrm{d}\theta} + \left(\frac{\lambda}{2}-1\right)\left(\frac{\lambda}{2}-2\right)\tilde{\tau}'_{rr\theta}\\
&+2\left(\frac{\lambda}{2}-1\right)\tilde{\tau}'_{\theta rr} - \left(\frac{\lambda}{2}-1\right)\tilde{\tau}'_{\theta\theta\theta} - \frac{\mathrm{d}\tilde{H}}{\mathrm{d}\theta} = 0,
\end{aligned} \tag{50}$$

where deviatoric stresses have been neglected because they are less singular than deviatoric higher-order stresses; $\tilde{H}(\theta)$ is the angular function of $H$, the combined measure of hydrostatic stress and hydrostatic higher-order stress, which has the asymptotic form

$$H = r^{(\lambda/2)-3}\tilde{H}(\theta) \tag{51}$$

near the crack tip. Eq. (50) provides two governing equations for the angular functions $\tilde{\phi}$ and $\tilde{H}$.

The traction-free boundary conditions (9) and (10) on the crack face can be written in polar coordinates as

$$\begin{aligned}
&\frac{\mathrm{d}\tilde{\tau}'_{\theta\theta r}}{\mathrm{d}\theta} + 2\left(\frac{\lambda}{2}-1\right)\tilde{\tau}'_{\theta rr} - \left(\frac{\lambda}{2}-1\right)\tilde{\tau}'_{\theta\theta\theta} = 0, && \text{at } \theta = \pi;\\
&\frac{\mathrm{d}\tilde{\tau}'_{\theta\theta\theta}}{\mathrm{d}\theta} + 2\left(\frac{\lambda}{2}-1\right)\tilde{\tau}'_{r\theta\theta} + \tilde{\tau}'_{\theta\theta r} - \tilde{H} = 0, && \text{at } \theta = \pi;\\
&\tilde{\tau}'_{\theta\theta r} = 0, && \text{at } \theta = \pi.
\end{aligned} \tag{52}$$

The other three boundary conditions are obtained from the symmetry (mode I) or anti-symmetry (mode II) conditions at the extended crack line $\theta = 0$. For mode I,

$$\tilde{\phi} = \tilde{\phi}'' = \tilde{\phi}^{(4)} = 0, \quad \text{at } \theta = 0; \tag{53}$$

while for mode II,

$$\tilde{\phi}' = \tilde{\phi}''' = \tilde{H} = 0, \quad \text{at } \theta = 0. \tag{54}$$

It should be pointed out that Eqs. (50), (52) and (53) for mode I or Eq. (54) for mode II form an eigenvalue problem, with $\lambda$ as the eigenvalue and $(\tilde{\phi}, \tilde{H})$ as the eigenvector. However, unlike the HRR field in classical plasticity (Hutchinson, 1968; Rice and Rosengren, 1968), the eigenvalue $\lambda$ is not known a priori.

Without losing generality, we may impose a normalization condition at $\theta = 0$. For mode I, this normalization condition can be stated as

$$\sqrt{\tilde{\phi}'(0)^2 + \tilde{\phi}'''(0)^2 + \tilde{H}(0)^2} = 1; \tag{55}$$

while for mode II, the normalization condition is

$$\sqrt{\tilde{\phi}(0)^2 + \tilde{\phi}''(0)^2 + \tilde{\phi}^{(4)}(0)^2} = 1. \tag{56}$$

The elimination of $\tilde{H}$ in the equilibrium equation (50) yields a sixth-order ordinary differential equation for $\tilde{\phi}$, which can be written as

$$\frac{\mathrm{d}^6\tilde{\phi}}{\mathrm{d}\theta^6} = \frac{g_1\left(\tilde{\phi}, \tilde{\phi}', \tilde{\phi}'', \tilde{\phi}''', \tilde{\phi}^{(4)}, \tilde{\phi}^{(5)}\right)}{g_2\left(\tilde{\phi}, \tilde{\phi}', \tilde{\phi}'', \tilde{\phi}'''\right)}. \tag{57}$$

For a mode II crack tip field, the anti-symmetry condition at $\theta = 0$ in Eq. (54) gives a vanishing denominator $g_2 = 0$. In fact, due to the anti-symmetry, $\tilde{\phi}$ can be expanded as a Taylor series of $\theta$ using only the even powers near $\theta = 0$. The denominator $g_2$ of Eq. (57) is on the order of $\theta$ near $\theta = 0$, while the numerator $g_1$ of Eq. (57) approaches a finite value $a_0$, where $a_0$ depends on $\tilde{\phi}(0)$, $\tilde{\phi}''(0)$ and $\tilde{\phi}^{(4)}(0)$. In order to have a finite derivative $\tilde{\phi}^{(6)}$ at $\theta = 0$ from the left-hand side of Eq. (57), the constant $a_0$ must vanish such that $\tilde{\phi}^{(4)}(0)$ is not independent of $\tilde{\phi}(0)$ and $\tilde{\phi}''(0)$. In conjunction with the normalization condition (56) for mode II, we find that both $\tilde{\phi}^{(2)}(0)$ and $\tilde{\phi}^{(4)}(0)$ are determined by $\tilde{\phi}(0)$. Therefore, there are only two parameters left, namely the power $\lambda$ and $\tilde{\phi}(0)$, to satisfy three traction-free boundary conditions (52) on the crack face. This is highly improbable to have solutions for two variables satisfying three equations. In fact, we have used the numerical shooting method (Press et al., 1986) to explore the entire range of $\lambda$ and $\tilde{\phi}(0)$, and indeed, no solutions can be found to satisfy three traction-free boundary conditions (52) on the crack face.

For a mode I crack tip field, $\tilde{\phi}$ becomes an odd function of $\theta$ due to symmetry. Accordingly, both $\tilde{\phi}^{(6)}$ from left-hand side and the numerator $g_1$ of Eq. (57) are zero at $\theta = 0$, while the denominator $g_2$ in (57) does not vanish. This observation, unlike mode II, does not result in an additional constraint among the boundary conditions at $\theta = 0$. The normalization condition (55) only gives $\tilde{H}(0)$ in terms of $\tilde{\phi}'(0)$ and $\tilde{\phi}'''(0)$. Therefore, there are three variables, namely the power $\lambda$, $\tilde{\phi}'(0)$ and $\tilde{\phi}'''(0)$, to satisfy three traction-free boundary conditions (52) on the crack face. We have also used the numerical

shooting method (Press et al., 1986) to search for solutions in the entire range of $\lambda$, $\tilde{\phi}'(0)$ and $\tilde{\phi}'''(0)$, and have reached the same conclusion that no solutions can be found for mode I.

The analysis in this section shows that the asymptotic crack tip fields in MSG plasticity do not have a separable form of solution, i.e., they cannot be written as $r^{\lambda}g(\theta)$ in polar coordinates $(r, \theta)$ as in the HRR field (1). It is quite puzzling why there is no separable form of solution. This is discussed in detail in the next section.

## 4. Discussion

All previous asymptotic fields around stationary crack tips have separable form of solutions as in Eq. (1), such as the classical $K$ field, HRR field (Hutchinson, 1968; Rice and Rosengren, 1968), crack tip field in the couple stress theory of strain gradient plasticity (Huang et al., 1995; Xia and Hutchinson, 1996), as well as the crack tip field in Fleck and Hutchinson's (Fleck and Hutchinson, 1997) phenomenological theory of strain gradient plasticity (Chen et al., 1999) (even though the last one has no domain of physical validity). These fields are all governed by the path-independent $J$-integral.

Unlike all asymptotic crack tip fields previously established, the asymptotic field in MSG plasticity does not have a separable form of solution. As we know, the asymptotic crack tip fields only hold within a small distance to the crack tip, typically 1/10–1/5 of the smallest relevant geometry or material length. In classical plasticity, there are no intrinsic material lengths such that the size of dominance zone of asymptotic field is governed by the crack length or plastic zone size. In phenomenological strain gradient plasticity, an intrinsic material length $l$ comes into play, scaling the strain gradients. Xia and Hutchinson (1996), Huang et al. (1997a, 1999a) and Chen et al. (1999) have shown that the dominance zone of asymptotic field indeed ranges from $l/20$ to $l/5$. In MSG plasticity, however, another material length, namely the mesoscale cell size $l_\epsilon$ given in Eq. (23), comes into play and scales the higher-order stresses. It is recalled that, for the separable form of asymptotic fields in Eqs. (24) and (39), higher-order stresses are more singular than stresses and become the dominating singular terms in equilibrium equations. Accordingly, $l_\epsilon$ becomes the smallest relevant length that governs the asymptotic crack tip field, and the dominance zone of the asymptotic field is roughly $l_\epsilon/10$. Gao et al. (1999) and Huang et al. (1999c) have estimated $l_\epsilon$ to be of the order of 10 times the average spacing among dislocations at plastic yielding, i.e., $\beta \sim 10$ in Eq. (23). For copper, Huang et al. (1999b) have established $l_\epsilon$ to be 500 nm. The size of the dominance zone of asymptotic field in MSG plasticity can be estimated as one-tenth of $l_\epsilon$, which becomes the average dislocation spacing at plastic yielding, and is of the order of 50 nm. This is not only outside the intended range of applications for strain gradient plasticity (0.1–10 μm), but also too small for any continuum plasticity theories to be applicable. This is because continuum plasticity represents a statistical average of the behavior of at least hundreds of dislocations, which are much larger than the aforementioned average dislocation spacing for the dominance zone of asymptotic crack tip field in MSG plasticity. It should be pointed out that even though the local density of dislocations around the crack tip might be larger than the average density in bulk materials such that this 50 nm may contain more dislocations than the above estimate of average dislocation spacing, 50 nm is still too small for the dominance zone of asymptotic field to contain enough dislocations for continuum plasticity to be applicable. For example, for a very high local density of $10^{16}$ $m^{-2}$, 50 nm contains only five dislocations. Therefore, even if the present analysis had given a mathematically separable solution as in Eq. (1), the solution would not have a domain of physical validity.

The fracture criterion (2) in classical plasticity is established from the existence of separable crack tip field such that the crack tip deformation is represented by a single amplitude factor $J$ as in Eq. (1). For MSG plasticity, however, such a separable crack tip field does not exist. What is the fracture criterion in MSG plasticity? Recent efforts in simulation of crack initiation and growth make use of an embedded

cohesive zone characterized by a work of separation and a separation strength (e.g., Needleman, 1987; Tvergaard and Hutchinson, 1992, 1993; Xu and Needleman, 1994; Camacho and Ortiz, 1996). Therefore, the cohesive law has replaced Eq. (2) to become the fracture criterion that is implicitly built into the continuum analysis. Gao and Klein (1998) and Klein and Gao (1998) have developed an alternative approach, namely the virtual-internal-bond (VIB) model, to build a fracture criterion into the continuum analysis. The VIB model with randomized internal cohesive interaction between materials particles has been proposed as an integration of continuum models with cohesive laws or atomistic models with interatomic bonding. It is different from the cohesive zone model in that continuum analysis and cohesive laws are integrated at the level of fracture process zone or finite element discretization. If the cohesive zone or VIB model is introduced in MSG plasticity, it is not necessary to establish an explicit fracture criterion as in Eq. (2).

In summary, the asymptotic crack tip field does not have a separable form of solution in MSG plasticity. Non-separable solutions for the crack tip field, in general, can be obtained numerically (e.g., by the finite element method).

## Acknowledgements

The work of Y. Huang was supported by the NSF through Grant CMS-9896285 and by the NSF of China. The work of H. Gao was supported by the NSF through Young Investigator Award MSS-9358093. The work of K.C. Hwang was supported by the NSF of China.

## References

Acharya, A., Bassani, J.L., 1999. Lattice incompatibility and a gradient theory of crystal plasticity, unpublished data.

Ashby, M.F., 1970. The deformation of plastically non-homogeneous alloys. Phil. Mag 21, 399–424.

Atkinson, M., 1995. Further analysis of the size effect in indentation hardness tests of some metals. J. Mater. Res 10, 2908–2915.

Begley, M.R., Hutchinson, J.W., 1998. The mechanics of size-dependent indentation. J. Mech. Phys. Solids 46, 2049–2068.

Camacho, G.T., Ortiz, M., 1996. Computational modeling of impact damage in brittle materials. Int. J. Solids Struct 33, 2899–2938.

Chen, J.Y., Huang, Y., Hwang, K.C., 1998. Mode I and mode II plane-stress near-tip fields for cracks in materials with strain gradient effects. Key Eng. Mater 145, 19–28.

Chen, J.Y., Wei, Y., Huang, Y., Hutchinson, J.W., Hwang, K.C., 1999. The asymptotic crack tip fields in strain gradient plasticity. Eng. Fracture Mech., in press.

Cottrell, A.H., 1964. The Mechanical Properties of Materials. Wiley, New York, p. 277.

Dai, H., Parks, D.M., 1998. Geometrically-necessary dislocation density in continuum crystal plasticity theory and FEM implementation, unpublished data.

de Guzman, M.S., Neubauer, G., Flinn, P., Nix, W.D., 1993. The role of indentation depth on the measured hardness of materials. Materials Research Symposium Proceedings 308, 613–618.

Elssner, G., Korn, D., Ruehle, M., 1994. The influence of interface impurities on fracture energy of UHV diffusion bonded metal–ceramic bicrystals. Scripta Metall. Mater 31, 1037–1042.

Fleck, N.A., Hutchinson, J.W., 1993. A phenomenological theory for strain gradient effects in plasticity. J. Mech. Phys. Solids 41, 1825–1857.

Fleck, N.A., Hutchinson, J.W., 1997. Strain gradient plasticity. In: Hutchinson, J.W., Wu, T.Y. (Eds.), Advances in Applied Mechanics, vol. 33. Academic Press, New York, pp. 295–361.

Fleck, N.A., Muller, G.M., Ashby, M.F., Hutchinson, J.W., 1994. Strain gradient plasticity: theory and experiments. Acta Metall. Mater 42, 475–487.

Gao, H., Huang, Y., Nix, W.D., Hutchinson, J.W., 1999. Mechanism-based strain gradient plasticity: Part I: Theory. J. Mech. Phys. Solids 47, 1239–1263.

Gao, H., Klein, P., 1998. Numerical simulation of crack growth in an isotropic solid with randomized internal cohesive bonds. J. Mech. Phys. Solids 46, 187–218.

Huang, Y., Chen, J.Y., Guo, T.F., Zhang, L., Hwang, K.C., 1999a. Analytical and numerical studies on mode I and mode II fracture in elastic-plastic materials with strain gradient effects. *Int. J. Fracture*, in press.

Huang, Y., Chen, J.Y., Guo, T.F., Zhang, L., Hwang, K.C., 1999b. Strain-gradient plasticity at the micron scale In: Ellyin, F., Provan, J.W. (Eds.). Prograss in Mechanical Behavior of Materials. Fleming Printing Ltd, pp. 1051–1056.

Huang, Y., Gao, H., Nix, W.D., Hutchinson, J.W., 1999c. Mechanism-based strain gradient plasticity. Part II: Analysis. J. Mech. Phys. Solids, in press.

Huang, Y., Zhang, L., Guo, T.F., Hwang, K.C., 1995. Near-tip fields for cracks in materials with strain-gradient effects. In: Willis, J.R. (Ed.), Proceedings of IUTAM Symposium on Nonlinear Analysis of Fracture. Kluwer, Cambridge, England, pp. 231–242.

Huang, Y., Zhang, L., Guo, T.F., Hwang, K.C., 1997a. Fracture of materials with strain gradient effects. In: Karihaloo, B.L., Mai, Y.W., Ripley, M.I., Ritchie, R.O. (Eds.), Advances in Fracture Research. Pergamon Press, Amsterdam, pp. 2275–2286.

Huang, Y., Zhang, L., Guo, T.F., Hwang, K.C., 1997b. Mixed mode near-tip fields for cracks in materials with strain-gradient effects. J. Mech. Phys. of Solids 45, 439–465.

Hutchinson, J.W., 1968. Singular behavior at the end of a tensile crack in a hardening material. J. Mech. Phys. Solids 16, 13–31.

Hutchinson, J.W., 1997. Linking scales in mechanics. In: Karihaloo, B.L., Mai, Y.W., Ripley, M.I., Ritchie, R.O. (Eds.), Advances in Fracture Research. Pergamon Press, Amsterdam, pp. 1–14.

Kannien, M.F., Popelar, C.H., 1985. Advanced Fracture Mechanics. Oxford University Press, Oxford, England.

Klein, P., Gao, H., 1998. Crack nucleation and growth as strain localization in a virtual-bond continuum. Engr. Fracture Mech 61, 21–48.

Kocks, U.F., 1970. The relation between polycrystal deformation and single-crystal deformation. Metall. Trans 1, 1121–1144.

Ma, Q., Clarke, D.R., 1995. Size dependent hardness of silver single crystals. J. Mater. Res 10, 853–863.

McElhaney, K.W., Vlassak, J.J., Nix, W.D., 1998. Determination of indenter tip geometry and indentation contact area for depth-sensing indentation experiments. J. Mat. Res 13, 1300–1306.

Needleman, A., 1987. A continuum model for void nucleation by inclusion debonding. J. Appl. Mech 54, 525–531.

Nix, W.D., 1989. Mechanical properties of thin films. Met. Trans 20A, 2217–2245.

Nix, W.D., 1997. Elastic and plastic properties of thin films on substrates: nanoindentation techniques. Mat. Sci. and Engr A234-236, 37–44.

Nix, W.D., Gao, H., 1998. Indentation size effects in crystalline materials: a law for strain gradient plasticity. J. Mech. Phys. Solids 46, 411–425.

Nix, W.D., Gibeling, J.C., 1985. Mechanism of time-dependent flow and fracture of metals. In: Metals/Materials Technology Series. ASM, Metals Park, OH, pp. 8313–8404.

Nye, J.F., 1953. Some geometrical relations in dislocated crystals. Acta Metall 1, 153–162.

Poole, W.J., Ashby, M.F., Fleck, N.A., 1996. Micro-hardness of annealed and work-hardened copper polycrystals. Scripta Metall. et Mater 34, 559–564.

Press, W.H., Flannery, B.P., Teukolsky, S.A., Vetterling, W.T., 1986. Numerical Recipes. Cambridge University Press, Cambridge.

Rice, J.R., 1968. A path-independent integral and the approximate analysis of strain concentration by notches and cracks. J. Appl. Mech 35, 379–386.

Rice, J.R., Rosengren, G.F., 1968. Plane strain deformation near a crack tip in a power law hardening material. J. Mech. Phys. Solids 16, 1–12.

Shu, J.Y., Fleck, N.A., 1998. The prediction of a size effect in micro indentation. Int. J. Solids Struct 35, 1363–1383.

Stelmashenko, N.A., Walls, A.G., Brown, L.M., Milman, Y.V., 1993. Microindentation on W and Mo oriented single crystals: an STM study. Acta Metall. et Mater 41, 2855–2865.

Stolken, J.S., Evans, A.G., 1998. A microbend test method for measuring the plasticity length scale. Acta Mater 46, 5109–5115.

Taylor, G.I., 1938. Plastic strain in metals. J. Inst. Metals 62, 307–324.

Tvergaard, V., Hutchinson, J.W., 1992. The relation between crack growth resistance and fracture process parameters in elastic–plastic solids. J. Mech. Phys. Solids 40, 1377–1397.

Tvergaard, V., Hutchinson, J.W., 1993. The influence of plasticity on mixed mode interface toughness. J. Mech. Phys. Solids 41, 1119–1135.

Wei, Y., Hutchinson, J.W., 1997. Steady-state crack growth and work of fracture for solids characterized by strain gradient plasticity. J. Mech. Phys. Solids 45, 1253–1273.

Xia, Z.C., Hutchinson, J.W., 1996. Crack tip fields in strain gradient plasticity. J. Mech. Phys. of Solids 44, 1621–1648.

Xu, X.-P., Needleman, A., 1994. Numerical simulations of fast crack growth in brittle solids. J. Mech. Phys. Solids 42, 1397–1434.